

RESEARCH

Open Access



Early embryonic development in the tick *Ixodes scapularis* suggests syncytial organization and cellularization before blastoderm formation

Isaac A. Hinne¹, Hailee R. Ciccotti¹, Jakub Wudarski¹, Michael N. Pham¹, Arvind Sharma¹, Molly M. McVicar¹, Benjamin Faustino¹, Andrew B. Nuss^{1,2}, Prashant P. Sharma³ and Monika Gulia-Nuss^{1*}

Abstract

Ixodes ticks are the most important vectors of arthropod-borne diseases in the United States, Canada, and Europe. *Ixodes scapularis* is the major vector that transmits the causative agent of Lyme disease in the eastern United States and can transmit up to six additional pathogens. In recent years, many advances have been made in building the toolkit for *I. scapularis* research, including genomic resources, transcriptomes, and forward and reverse genetics techniques. However, an understanding of the early embryonic development of this species is still lacking. In this study, we attempted to fill this knowledge gap and to further the efforts of functional genomics tools development. We developed a staging system consisting of 16 (0–15) stages describing unique morphologies and used wheat germ agglutinin staining and fluorescent dye injections to confirm cell membrane formation. These results provide an opportunity to identify an ideal time window for tick transgenics and deepen our understanding of the events during embryo development.

Keywords Chelicerate, Ticks, Embryogenesis, Syncytial blastoderm, Cellularization

Introduction

Ticks are vectors of medical and veterinary importance and can transmit a variety of pathogens, including viruses, bacteria, protozoans, and fungi [1]. Ticks and the diseases they transmit incur significant costs to public health and agriculture worldwide [1]. For instance, *Ixodes scapularis* alone is estimated to be responsible for over 500,000 Lyme disease cases annually [2] and may transmit

six other pathogens, including species of *Anaplasma*, *Babesia*, *Ehrlichia*, *Rickettsia*, and Flaviviruses [1, 3, 4].

Due to the lack of genetic transformation tools, research on tick molecular biology and host–pathogen interactions has been severely limited. Our recent work has permitted us to overcome this impediment by developing an embryo injection protocol [5, 6]. Effective genetic transformation requires knowledge of early embryonic events, principally the timing of cellularization and/or localizing germ cells within the developing embryo. This knowledge is essential so that the introduced material can access the nucleus (before cellularization) of the primordial germ cells (pole cells) and create stable germline transformants.

The reproductive system of ticks is different from well-studied arthropod models such as *Drosophila melanogaster*. For instance, tick ovaries are panoistic and the oocytes attach to the ovarian wall by pedicel

*Correspondence:

Monika Gulia-Nuss
mgulianuss@unr.edu

¹ Department of Biochemistry and Molecular Biology, University of Nevada, Reno, USA

² Department of Agriculture, Veterinary, and Rangeland Science, University of Nevada, Reno, USA

³ Department of Integrative Biology, University of Wisconsin, Madison, USA



© The Author(s) 2025. **Open Access** This article is licensed under a Creative Commons Attribution-NonCommercial-NoDerivatives 4.0 International License, which permits any non-commercial use, sharing, distribution and reproduction in any medium or format, as long as you give appropriate credit to the original author(s) and the source, provide a link to the Creative Commons licence, and indicate if you modified the licensed material. You do not have permission under this licence to share adapted material derived from this article or parts of it. The images or other third party material in this article are included in the article's Creative Commons licence, unless indicated otherwise in a credit line to the material. If material is not included in the article's Creative Commons licence and your intended use is not permitted by statutory regulation or exceeds the permitted use, you will need to obtain permission directly from the copyright holder. To view a copy of this licence, visit <http://creativecommons.org/licenses/by-nc-nd/4.0/>.

cells, cells analogous to the follicle and nurse cells of insect ovaries [7]. The paired *Ixodes* ovaries are thin-walled and tubular, consisting of epithelial cells overlying a 4–5-layer fibrous basal lamina [8]. Primary oocytes first appear in fed nymphs and become arrested in an early stage of development. Vitellogenesis begins only after the female engorges with blood. During the first few days of blood feeding, arrested oocytes resume development by expanding their cytoplasm and enlarging their nucleus [9]. Insemination and complete engorgement generally are prerequisites for continued deposition of yolk [9]. Egg shells are secreted by the oocyte itself and lack a true micropyle [10]. Completion of development is asynchronous, with oocytes in many different developmental stages simultaneously present in the ovaries. Eggs accumulate in the lumen of the ovary and oviduct as ovulation proceeds. The cuticle surrounding the genital pore rearranges itself for egg laying and opens anteriorly facing the vertically oriented capitulum. This repositioning facilitates the exposure of eggs to Gene's organ, an eversible multilobed gland [11]. Eggs are released due to peristaltic contractions of the cervical vagina through the genital pore via the prolapsed vestibular vagina. The legs and mouth parts facilitate wax coating by the lobes of Gene's organ that protrude to coat newly released eggs with wax to minimize desiccation. Syngamy has been shown to take place in the oviducts of soft ticks [12]. However, the precise site of fertilization in hard ticks remains to be established.

Tick eggs are spherical to ovoid-oblong. No orientation (dorsal, ventral, or lateral) is readily evident in the early stages of embryo development. In insects, the initial cues required to determine the anteroposterior (AP) and dorsoventral (DV) axes are established during oogenesis. In the fruit fly *D. melanogaster* and the beetle *Tribolium castaneum*, the DV axis is established through maternal interactions among epidermal growth factor, Toll, and bone morphogenetic protein (BMP) pathways [13–15]. In contrast, the AP and DV axes in spiders, another chelicerate, are established by zygotic gene interactions followed by the migration of the cumulus, a specialized group of cells [16–18]. In spiders, cumulus mesenchymal cell migration requires the secreted factor decapentaplegic (Dpp), a BMP homolog, and this movement is essential for the determination of the DV axis [16, 19]. BMP activity was also detected in a specific cell population in the cattle fever tick, *Rhipicephalus microplus* [20] suggesting that spiders and ticks likely have similar embryonic axis development and it differs from the insect models.

Studies on tick embryonic development in genera such as *Dermacentor* [21, 22] and *Rhipicephalus* [20,

23] have been conducted in some detail; however, information on several aspects of embryonic development such as whether initial development is via a syncytium or a holoblast are still missing. Santos et al. [20] developed the tick embryo staging system for *R. microplus* based on spider embryogenesis [24–26]. However, the youngest embryos used for staging were 24 h after egg laying (hAEL), and early development (before 24 hAEL) in this genus has yet to be described. In the absence of an embryo injection protocol, the authors used pTyr antibody staining to visualize cell membrane formation and concluded that the cellularization occurs early in tick development (within 24 hAEL in this species). However, Campos et al. [23], using similar rearing conditions, suggested that until 5 days after egg laying (dAEL), the *R. microplus* embryo is a syncytium (a single cell containing several nuclei, formed by nuclear division), and cellularization occurs at 6 dAEL. Because of these conflicting results, early nuclear and cellular divisions need to be confirmed in ticks. Except for an embryonic development study on *Ixodes calacaratus* [27] (later synonymized with *Rhipicephalus annulatus*), published over a century ago in Russian, no other description of the embryonic development of any member of the genus *Ixodes* appears in the literature [28].

Total cleavage is considered the rule during embryogenesis among the *Ixodidae*, mainly based on one ultrastructural study of the soft tick, *Ornithodoros moubata* [29]. Whether or not the early divisions in tick embryos are holoblastic (with mitosis and cytokinesis) or syncytial (nuclear division only) remains to be confirmed.

Based on morphological differences, hard ticks, *Ixodidae*, are divided into the Metastriata and the Prostriata. In the United States, *Ixodes*, *Amblyomma*, *Dermacentor*, and *Rhipicephalus* are the major genera of human health significance. *Ixodes* is the only genus representative of the Prostriata, whereas the latter three genera are members of the Metastriata. While embryonic staging systems have been studied to some extent for metastriate ticks, embryonic staging for prostriate ticks is lacking. Here we have established an embryonic staging system for *I. scapularis* consisting of 16 stages. We added a new stage 0 to the previously described stages in other tick species. We investigated the timing of cellularization by injecting dextran conjugated with Alexa Fluor and also stained fixed embryos with wheat germ agglutinin. Together, our data supports a syncytium that lasts up to 3 days after egg laying before the blastoderm formation. The staging and precise description of embryonic events will facilitate further studies on this medically important

vector species and support the development of new genetic tools for tick research.

Results

Egg laying

Females in the colony fed on rabbits for approximately 6 days before falling off. Replete females were collected daily and kept at 20 °C in individual vials. The engorged females begin laying eggs 7–8 days post-drop-off and deposit eggs singly every 2–5 min when undisturbed (Movie S1).

Embryonic stages

The proposed staging for *R. microplus* [20] provided the basis for the present staging scheme of *I. scapularis* to achieve a standardized staging system for ticks. As *R. microplus* embryonic development time is much shorter (15–20 days) than *I. scapularis* (35–40 days), the stages differ in time. We also defined new stages by analyzing early embryos (0–5 hAEL). As a general overview, we provide a table containing all developmental stages of *I. scapularis* based on DAPI staining (Table 1). The embryos were kept at 20 °C.

Stage 0 (< 5 hAEL), no visible nucleus

Ixodes scapularis eggs are ellipsoidal with a diameter of approximately 200 µm and contain a large quantity of homogenous yolk. No nuclei were visible via either DAPI staining between 0 and 5 hAEL or the timelapse images. This was termed stage 0 (Table 1, Fig. 1A, Movie S2). This stage was established to account for an earlier time point that was not characterized in earlier studies [20, 21].

Stages 1–3 (5 h–3 dAEL): rapid nuclear division without cellularization

Stage 1 (Fig. 1B) likely started 4–5 hAEL when a single nucleus became visible by DAPI staining in the center of the egg. The first cleavage occurs deep within the center of the yolk sometime after 2 hAEL. Because cleavage of energids (nuclei and their surrounding cytoplasm) are within the heavily dense yolk and have not yet migrated cortically, one nucleus with DAPI stain was observed at 6 hAEL (Fig. 1B). However, four cleavage energids were visible between 6 and 12 hAEL in the timelapse images (Fig. 1B; Movie S2; Movie S3 frames 1–11). The timelapse images suggest syngamy might occur in the first hour after egg laying (Movie S2). The first few cleavages appear to be synchronous.

Stage 2 begins at 12 hAEL and ends at approximately 2 dAEL. At this stage, the energids begin to divide rapidly in the center of the egg and start moving towards the periphery (Fig. 1C, D; Movie S3 frame 12). The nuclear division is faster at this stage.

Stage 3 began and ended at 3 dAEL. At this stage, nuclei reached the surface of the egg and cleavage continued (Fig. 1D). These energids were connected with the cortical periplasm by thin projections along yolk columns at the surface of the egg (Movie S4 frames 1–23). The cleavage at this stage was meroblastic i.e., nuclear division without cytokinesis, and most likely asynchronous, resulting in a multinucleated syncytial embryo. In some embryos, pairs of nuclei were observed in proximity or segregating during mitotic telophase (Fig. 1D, D'). Cleavage in this embryo was different from the syncytial blastoderm of *D. melanogaster*. The energids were not part of a continuous layer of superficial cytoplasm but were separated from one another by densely packed yolk granules that extended to the surface of the egg. Neighboring nuclei were not in mitotic synchrony, suggesting that the functional interactions between them were much looser than between the syncytial nuclei of *D. melanogaster*, which undergo coordinated waves of mitosis [30].

Stage 4 (4–5 dAEL): blastoderm and cellularization

At stage 4 (4–5 dAEL), continued mitosis led to the proliferation of nuclei at the surface of the embryo to establish a relatively uniform blastoderm (Fig. 2A). Heavy contractions within the yolk granules were also observed (Movie S3 frames 65–111). These contractions may have been a sign of cellularization. We further confirmed cellularization in two ways: (1) embryos injected with a dextran-conjugated fluorescent dye (Dextran-Alexa Fluor 647) and (2) labeled fixed embryos with wheat germ agglutinin (WGA) conjugated to fluorescein isothiocyanate (FITC). Both datasets corroborated and suggested cellularization by 4 dAEL. These results are shown later in this section (Figs. 6, 7).

Stage 5 (6–7 dAEL) gastrulation and cumulus formation

Stage 5 began at 6 dAEL and lasted until 7 dAEL. This stage was characterized by the formation of a distinct germ disc in one hemisphere of the egg (Movie S2). The heavy contractions within the yolk became more localized at a region close to the surface of the egg where an indentation and a denser spot of cells appeared, which was likely the site of gastrulation (blastopore) (Fig. 2B, Movie S3 frame from 285, Movie S4). An agglomerate of internalizing cells which may be likened to the primary thickening observed in spiders [19, 26, 31] was also seen at this stage (Movie S3 frame from 295 to 350). In later stages, we observed these cells “move” to the posterior of the germ band, but this movement seems to be a result of embryo inversion to internalize the yolk (Movie S3 frames 492–548).

Table 1 Developmental stages, times, and events of *Ixodes scapularis* embryogenesis

Developmental stage	Time in hours (h) or days (D)	Event
0	0–4 h	No nucleus visible
1	5–12 h	Early nuclear division in the yolk, energids visible
2	12 h–2D	Nuclear migration to the periphery of the egg
3	2–3 D	Nuclear division at the periphery of the egg
4	3–5 D	Cellularization, Blastoderm formation
5	6–7 D	Gastrulation, Cumulus formation
6	9–10 D	Dorsal field, cell migration to poles
7	10–11 D	Germ band formation

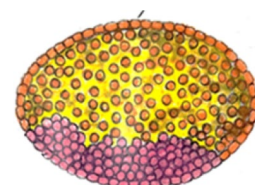
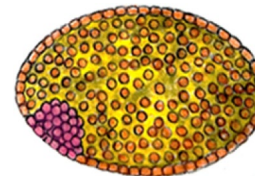
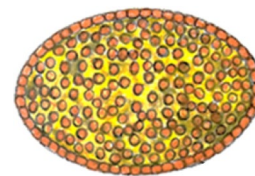
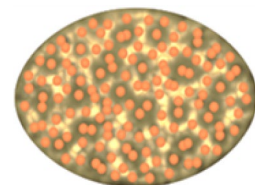
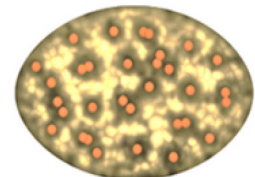
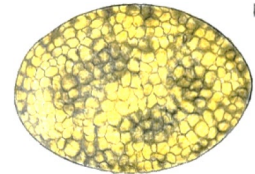
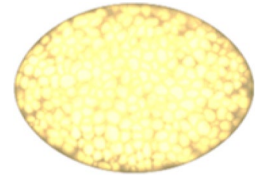


Table 1 (continued)

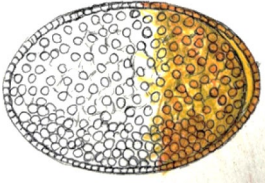
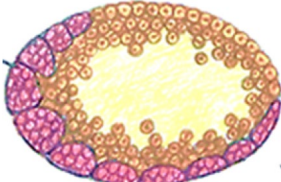

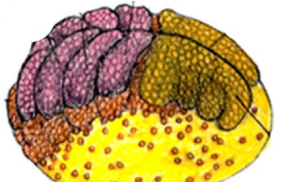
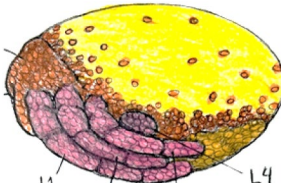


Developmental stage	Time in hours (h) or days (D)	Event	
8	12 D	Perivitelline space, Inversion, Ventral furrow	
9	12–13 D	Germ band segmentation and extension	
10	13–14 D	Budding appendages, the tube-like structure extends from the growth zone (post-abdomen)	
11	15–16 D	Extending appendages, germ band contraction	
12	17–18 D	Extending appendages, 4th leg retracts, Dorsal closure begins	
13	20–27 D	Ventral closure, Malpighian tubules transport waste to the rectal sac	
14	28–35 D	Embryo rotates to the final position. All external structures are in the final position. Idiosoma (fused podosoma and opisthosma) and capitulum, palps, hypostome, and chelicerae are fully developed. Last pair of legs (L4) retracted, and three leg pairs (L1-L3) fully elongated and segmented; Haller's organ and sensory structures visible	

Table 1 (continued)

Developmental stage	Time in hours (h) or days (D)	Event
15	35–40 D	Dorsal closure complete, Cuticle deposition, hatching



The stages are Based on staging in *Rhipicephalus microplus* [20] and *Dermacentor andersoni* (Freisen et al. 2016). Intervals are reported in hours and days after egg laying. Embryos were held at 20 °C and 95% RH

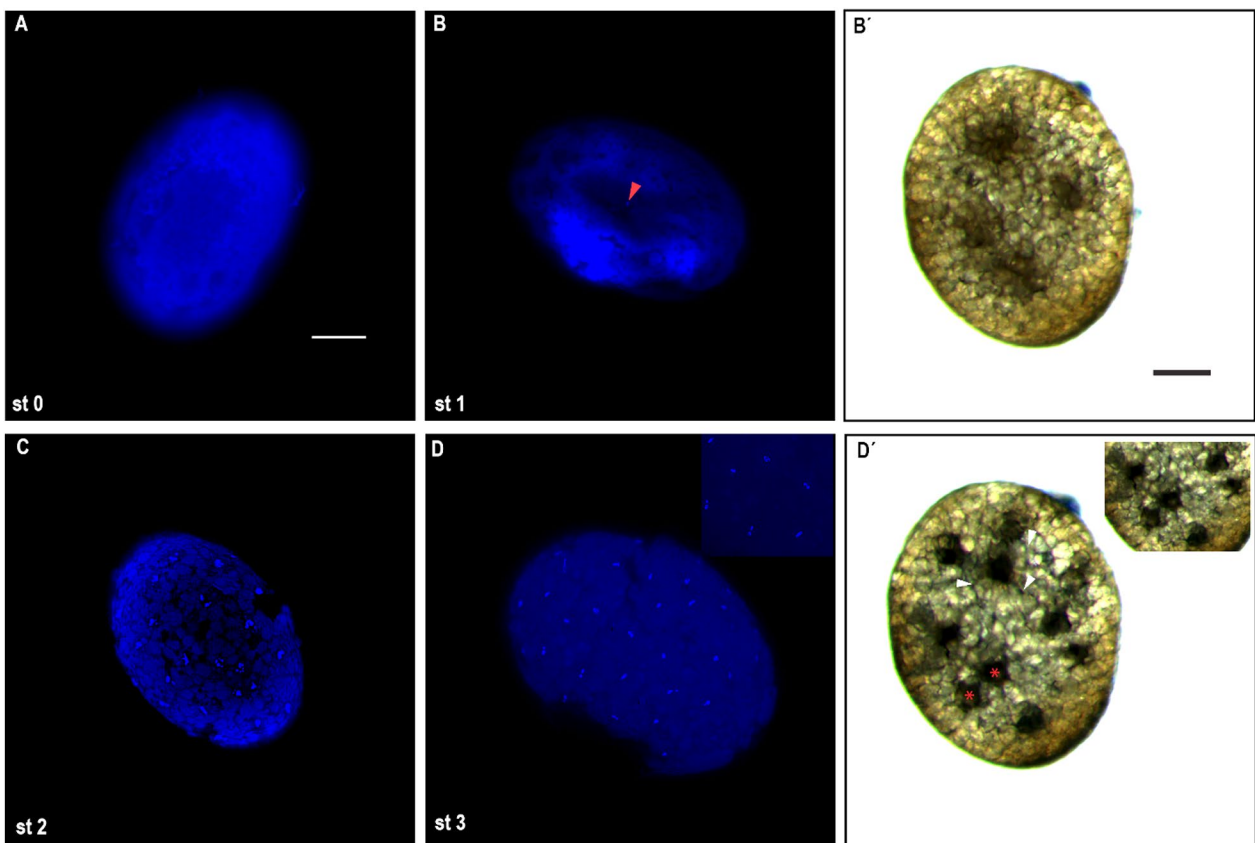


Fig. 1 DAPI stained images and stills from time-lapse imaging of Stages 0 to 3. DAPI-stained images of stages 0 to 3 (**A–D**). Stills from time-lapse imaging (**B'** and **D'**). **A** Stage 0, no nucleus visible. **B, B'** Stage 1: early nuclear/energid division within the yolk (red arrowhead in B). Energid division at this stage appears to be synchronous. **C** Stage 2: nuclei have migrated to the periphery of the egg. **D, D'** Stage 3: asynchronous nuclear division. The energids with red asterisks are dividing while the neighboring energids are not (see a zoomed image in insert). All the energids are connected and the periphery of the egg via thin stands (white arrowheads). Scale bars are 100 μ m. st: stage

Stage 6–8 (8–12 dAEL): dorsal field, germ band formation, embryo inversion

Stage 6 (8–9 dAEL) was marked by the establishment of a dorsal field where nuclei migrated away from and became concentrated at the ventral side (Fig. 2C). These nuclei extended to the poles to form the ventral germ

band, which lies along the longitudinal axis by stage 7 (10–11 dAEL) (Fig. 2D). The dorsal field, which is opposite the ventral germ band, became distinct with a lower concentration of nuclei. The embryo contracted and a perivitelline space becomes visible at both vertices of the embryo, which marked the beginning of stage 8 (12

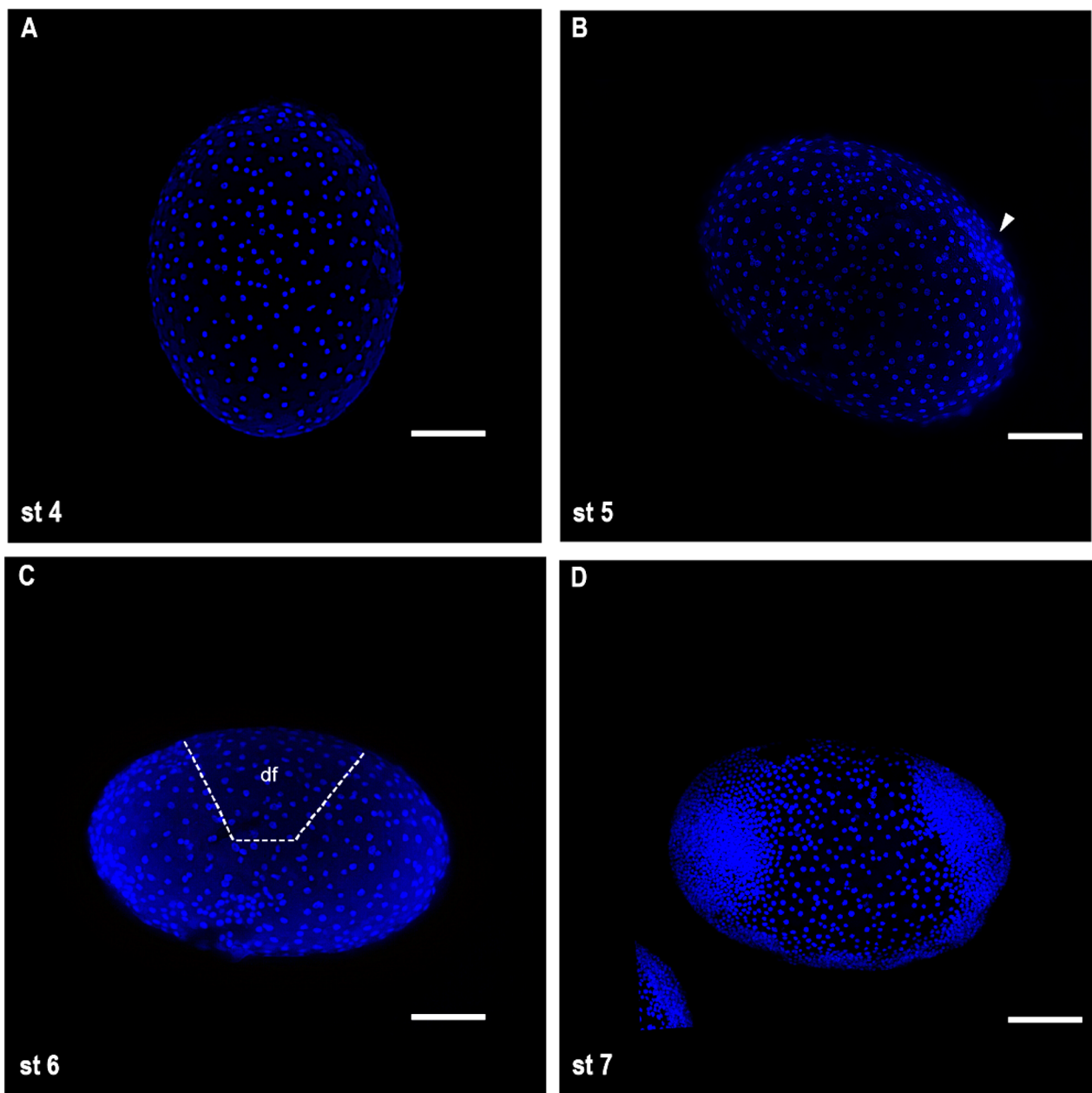


Fig. 2 DAPI stained images of stages 4 to 7. **A** Stage 4: continued mitosis leads to the formation of blastoderm. **B** accumulation of a group of cells at one side of the egg (white arrowhead) at Stage 5. **C** Stage 6: the cells begin to move to the poles creating a dorsal field (dashed lines, df) with fewer cells. **D** Stage 7: the cells have accumulated at the poles and the ventral side of the egg to form a ventral germband. Scale bars are 100 μm , st: stage, df: dorsal field

dAEL) (Fig. 3A and Movie S3 frames 410–515). The embryo took on a horseshoe appearance during the contraction, and inversion occurred to internalize the yolk, during which the ventral germband split into two halves during late stage 8 (Movies S3 frames 488–557, S3 frames 1530–1738).

Stages 9–10 (13–15 dAEL): germ band segmentation, extension, budding appendages

At stage 9 (13–14 dAEL), segmentation of the germ band became apparent as more cells became concentrated in the segments with visible grooves (Fig. 3B). The dense spot of cells was still visible at the pole region that would become the posterior pole (Fig. 3B). Only at this stage did the anterior and posterior ends become apparent (Movie

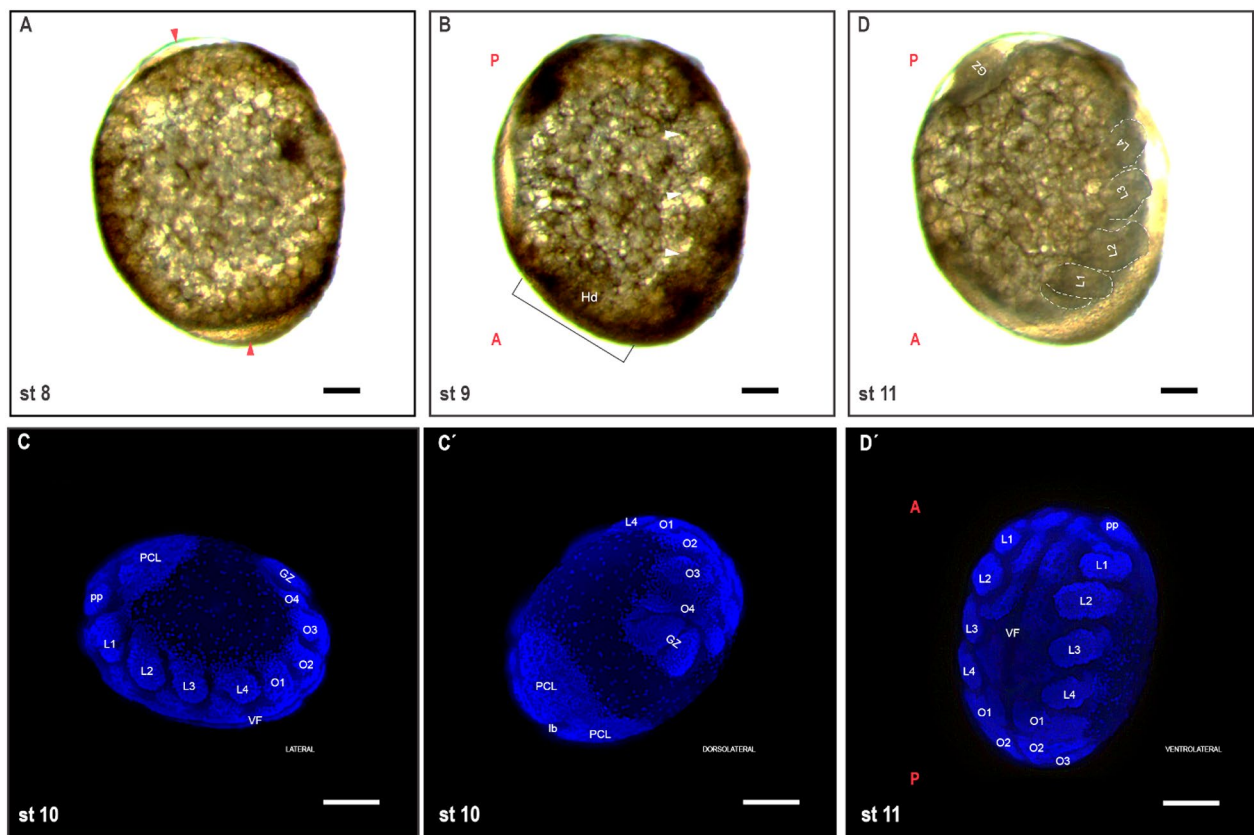


Fig. 3 DAPI stained images and stills from time-lapse images of stages 8 to 11. **A** Stage 8: perivitelline space (red arrowheads) forms at both poles of the embryo and allows embryo inversion to occur during which the embryo splits into two halves creating the ventral furrow. **B** Stage 9: the germ band is fully extended and segmental grooves (white arrowheads) are visible. It is at this stage that true anterior and posterior ends are defined. **(C, C')** Stage 10: lateral and dorsolateral views of the same embryo at Stage 10. During this stage, prosomal and opisthosomal segments are visible. Appendages primordia begin to form. **(D, D')** Stage 11: germ band retraction begins and appendages start to elongate. A—anterior; P—posterior; L1–L4—Budding legs 1–4; O1–O4—opisthosomal segments; PCL—pre-cheliceral lobe, pp—budding pedipalps; lb—labium; Hd—head region; V—ventral furrow/sulcus; GZ—growth zone (post-abdomen). Scale bars are 100 μm . st: stage

S4 frame 559) as there was clear segmentation in the prosoma (anterior) and opisthosoma (posterior) regions at this stage (Fig. 3B).

At stage 10 (15 dAEL), the anterior pre-cheliceral lobes (PCL) region was visible, and the posterior was clearly defined, with the primary thickening making the posterior-most part (Fig. 3C, C'). The anterior and posterior regions were in proximity to the dorsal side of the embryo, marking a complete extension of the germ band. Shortly after, pairs of legs and mouth appendages emerged ventrolaterally from the germ band, marking the beginning of the appendage formation. There were four leg pairs (L1–L4) and a pair of pedipalps (pp) anterior to the first pair of legs are visible (Fig. 4C). Four opisthosomal segments (O1–O4) were also visible posterior to the fourth leg pair (Fig. 3C, C'). Right before the legs began to bud, the group of cells, which ended at the extreme posterior of the growth zone, began to invaginate to form the proctodeal cavity, which marked the initiation of hindgut

development (Movie S3 frame 600). During the invagination, a tube-like structure bulged outward, oriented away from the egg, similar to what has been described as post-opisthosoma or “post-abdomen”, a term that was coined by Holm [32] (Movie S3 from frame 630, Movie S4 from frame 1985). The ventral furrow was still open at this stage.

Stages 11–12: (16–18 dAEL) germ band retraction, extending appendages, dorsal closure

Stage 11 (16 dAEL) was characterized by the onset of germ band retraction and appendage elongation (Fig. 3D, D'). The post-abdomen at the extreme posterior began to move away from the dorsal to the ventral side of the embryo (Fig. 3D, (Movie S3 from frame 741, S4 from frame 2183). During this stage, the growth zone was fully extended, and appendages (legs and pedipalps) began elongating through cellular proliferation, with all four leg pairs appearing comparable in size and tube-like in

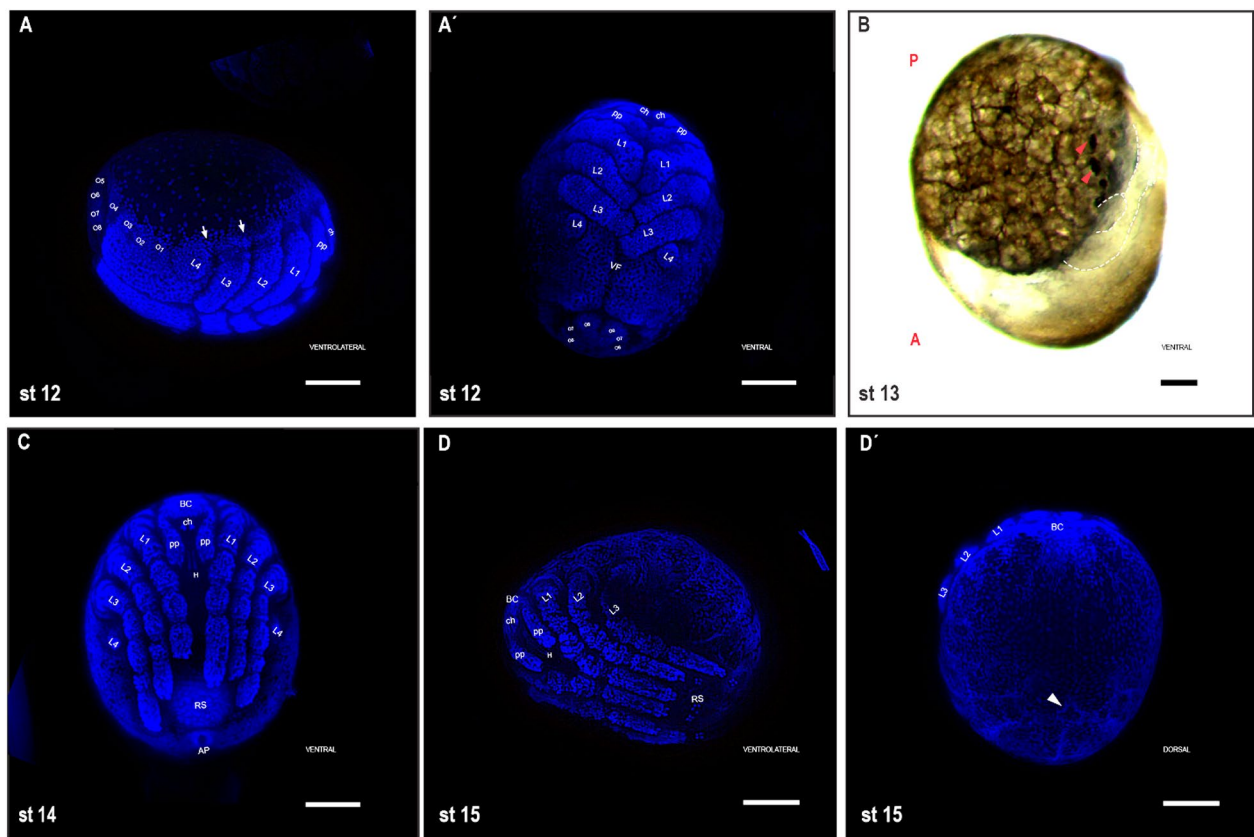


Fig. 4 DAPI stained images and stills from time-lapse imaging of stages 12 to 15. **A, A'** Stage 12: germband retraction continues and the post-abdomen moves further away from the dorsal side. The 4th leg pair retracts while the other limbs continue to develop. The post-abdomen bears four additional segments (O5 to O8) (**A**). The ventral furrow is still open. The pedipalps are bifurcated to form endites. Cells move from the opisthosoma (white arrows) to begin dorsal closure (**A'**). **B** Stage 13: the post-abdomen moves to the ventral, unfolds and the proctodeum becomes the anus. Waste substances (red arrowhead) begin moving to the rectal sac via the malpighian tubules. **C** Stage 14: the embryo has retracted to the anterior region. The ventral furrow is closed. The pre-cheliceral lobe has retracted to form the basis capitula. All appendages are formed and have moved to their final positions. **D, D'** Stage 15: cuticle synthesis and deposition begin. The embryo darkens from cuticle deposition. The dorsal cells meet up and form a ring structure (arrowhead) where final dorsal closure occurs. A—anterior; P—posterior; L1–L4—Budding legs; O—opisthosomal segments; PCL—pre-cheliceral lobe, pp—budding pedipalps; lb—labium; Hd—head region; VF—ventral furrow/sulcus; RS – rectal sac; AP—anal pore; BC—basis capitula; H—hypostome; ch—chelicerae. Scale bars are 100 μ m

shape (Fig. 3D'). Four additional segments (O5–O8) were visible with DAPI stain on the post-abdomen (Fig. 4A, Movie S4 frames 2611–3177).

By stage 12 (17–18 dAEL), the 4th leg pair stopped extending and began to retract while the remaining limbs developed (Fig. 4A). As the germ band retracted further, the post-abdomen moved further away from the dorsal towards the ventral side (Fig. 4A'). Podomerization of the legs began and the pedipalps became bifurcated (to form endites) (Fig. 4A, A'). Cells from the prosoma and opisthosoma began migrating dorsally to initiate dorsal closure by day 17 (Fig. 4A arrows). The post-abdomen settled near the ventral side and unfolded to form the posterior region (Movie S3 frames 950–1028, S4 frames 3000–3177), where

the proctodeal pore formed the anal pore and moved further at the ventral-posterior side to its final position by day 18. The retraction of the germ band brought the legs closer to the anterior region, and they continued to elongate towards the anal pore.

Stages 13–15: (19–40 dAEL) ventral closure, rectal sac formation, cuticular formation, larval hatching

During stage 13 (19–22 dAEL), the ventral sulcus closed transiently to bring the two halves of the embryo together and dorsal closure was also completed. This longer developmental stage was marked by a clearly defined ventral closure that separated it from future stages (Fig. 4B). Small dark masses (waste) (Movie S3 from frame 1144) were being transported through the

Malpighian tubules to the rectal sac at the ventral-posterior side of the embryo, creating a visible dark solid mass, a guanine spot (Movie S3 from frame 1370).

Stage 14 (23–30 dAEL) was marked by the rotation of the embryo to its final position within the vitelline membrane (Movie S3 frames 1348–1553). All prosomal and opisthosomal structures had formed and reached their final positions. The bifurcated palps and chelicerae were fully developed and in the final position. The hypostome was also in its final position. The fourth leg pair (L4) was nearly fully retracted, while the other three (L1–L3) were fully elongated and segmented (Fig. 4C).

Stage 15 (31–40 dAEL) was characterized by the synthesis and deposition of chitinous cuticle during which the embryo darkened and DAPI staining to mark nuclei became difficult (Fig. 4D, D'). L4 was fully retracted, and Haller's organs were visible on the first pair of legs (Movie S3). The dorsal cells formed a ring-like structure where the final dorsal closure occurs (Fig. 4D'). As hatching approached, the larva began to twitch repeatedly and strikes its legs against the walls of the vitelline membrane, eventually breaking the membrane and emerging (Movies S3 frames 2544–2920, Fig. 5).

Cellularization

Utilizing our embryo injection protocol [5, 6], we injected *I. scapularis* embryos with a dextran-conjugated fluorescent dye (Dextran-Alexa Fluor 647) in embryos. We tested the hypothesis that the absence of cell membranes would provide an ideal environment for the diffusion of

the dextran molecules. We observed complete dye diffusion in 2 dAEL (stage 3) injected embryos (Fig. 6A). At 3 dAEL, dye was more visible at the periphery suggesting the initiation of the cytokinesis (Fig. 6B). In contrast, 4 dAEL eggs showed localized dye at the injection site (Fig. 6C), suggesting complete cytokinesis.

To further our results with injected Dextran dye, we used wheat germ agglutinin (WGA) conjugated to fluorescein isothiocyanate (FITC) to label cell membranes. WGA binds glycoproteins containing N-acetylglucosamine and sialic acid residues, predominantly found on plasma membranes, and has been used to label cell membranes in live cells and animals as well as fixed cells [33]. We labeled fixed tick embryos with WGA-FITC and DAPI. WGA-labeling of cell membranes was observed at 4–5 dAEL (Fig. 7). Labeling live embryos by injecting WGA-FITC was unsuccessful.

Validation of cumulus-like cell formation

In chelicerates, the regulation of bone morphogenetic protein (BMP) signaling by cumulus mesenchymal cells defines dorsal–ventral (DV) axes by breaking the radial symmetry of the embryo. The cumulus is a cluster of cells that arise from one side of the primary thickening and migrate to the rim of the germ disc. During this migration, the cumulus cells express *decapentaplegic* (*dpp*) which induces BMP activity in the overlying epithelial cells, causing them to become dorsal cells.

DAPI staining at stage 5 (6–7 dAEL) revealed a cluster of cells (Fig. 3B) that we presumed to have cumulus

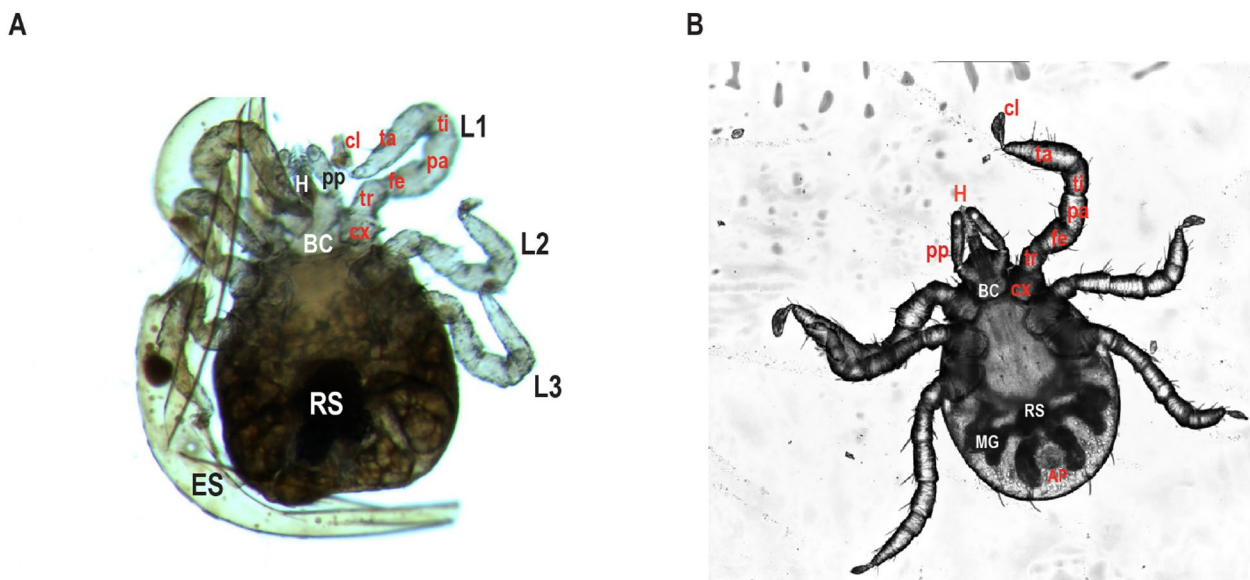


Fig. 5 Hatched larva. The larva hatches by breaking the eggshell. **A:** newly hatched larva. **B:** one-month-old larva. BC—basis capitulum, ES—eggshell, RS—rectal sac, H—hypostome, pp—pedipalps, L1–3—leg 1–3, cx—coxa, tr—trochanter, fe—femur, pa—patella, ta—tarsus, ti—tibia, cl—claw

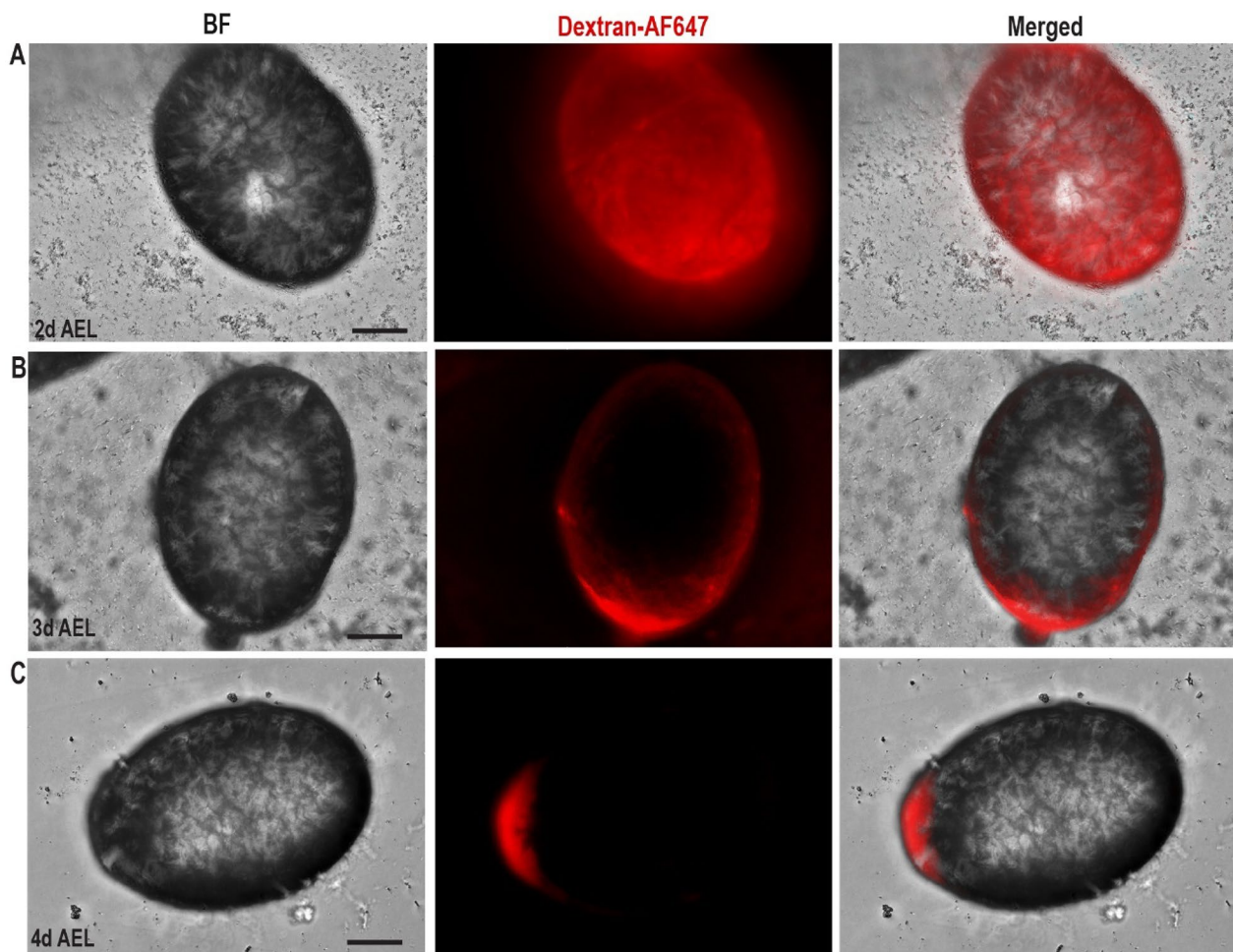


Fig. 6 Dextran Alexa fluorophore injection in embryos to determine cell membrane formation. Live embryos were injected with Dextran-AF 647 and were imaged 16 h post-injection. **A** in embryos, 2 dAEL dextran spreads through the entire embryo as shown by the fluorescence. **B** At 3 dAEL dextran is restricted to the peripheral regions of the embryo **C** At 4 dAEL dextran is restricted to the injection site signifying cellularization has occurred. dAEL- days after egg laying. Scale bars are 100 μ m

mesenchymal cells. Using antibody staining against the phosphorylated Mothers against dpp (pMAD) as has been done in other arthropods [16, 17, 19, 20], we detected BMP activity in a cluster of cells beneath the surface of the epithelial layer in eggs 6 dAEL (Fig. 8A), which confirms the presence of cumulus cells. By stage 7, pMAD staining was spread around the ventral germband and wasn't localized (Fig. 8B).

Discussion

Among the major unaddressed questions in tick embryology is whether ticks undergo total cleavage or form a syncytium during early embryonic development, as well as the timing of cellularization [20, 23, 29]. Here,

we offer insight into these previously unanswered questions.

Ixodes scapularis embryos exhibit the same general developmental pattern and morphogenetic processes as the related ixodid tick, *R. microplus* [20] and *D. andersoni* (Friesen et al., 2015). However, due to longer embryonic development in *I. scapularis*, stages are extended. *Ixodes scapularis* embryonic development is between 35 and 40 days, whereas *R. microplus* (~21 days) [20] and *D. andersoni* (14–18 days) [21] have much shorter developmental times. Therefore, the ages for each stage from previous research were not used in this work, instead, they were determined experimentally. Furthermore, the descriptions of each stage, apart from stage 0, were utilized to determine the morphological changes in embryos. Where possible, the staging system was kept consistent with the previous work.

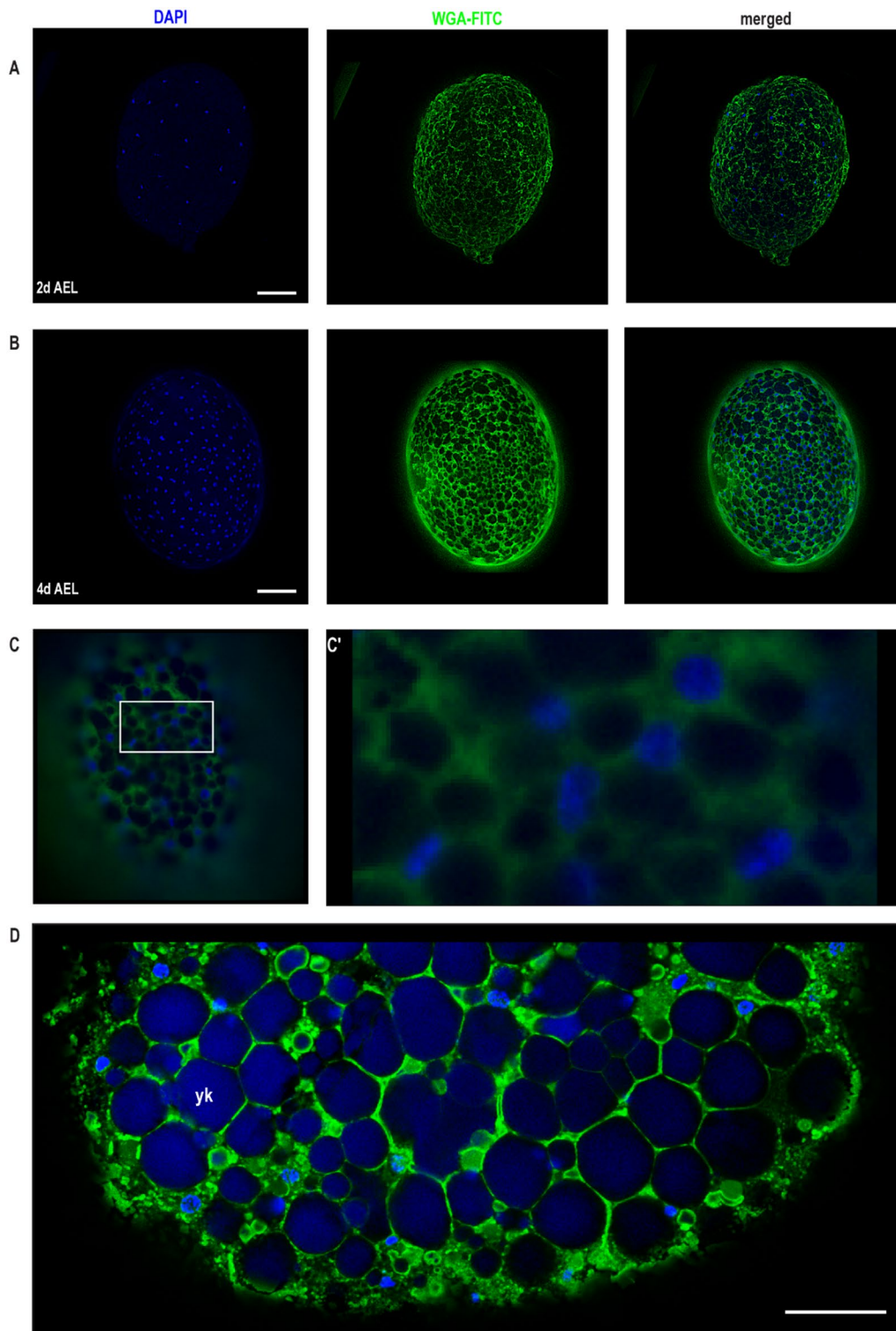


Fig. 7 Cell membrane formation in early *I. scapularis* embryos via Wheat Germ Agglutinin staining. Fixed eggs were stained with WGA-FITC and counterstained with DAPI. **A** Eggs two days after egg laying (2 dAEL) had no signs of membranes forming around the nuclei. **B** At 4 dAEL, cell membranes have formed around the nuclei. **C** Single optical slice from Keyence microscopy of 4 dAEL embryos. **C'** a zoomed section showing membrane formation around nuclei. **D** Single optical slice from confocal scans (maximum intensity projection) of 4 dAEL embryo showing the membrane formation around nuclei and yolk granules from excessive DAPI stain. yk – yolk, dAEL- days after egg laying. Scale bars are 100 μ m (**A-C**) and 50 μ m in (**D**)

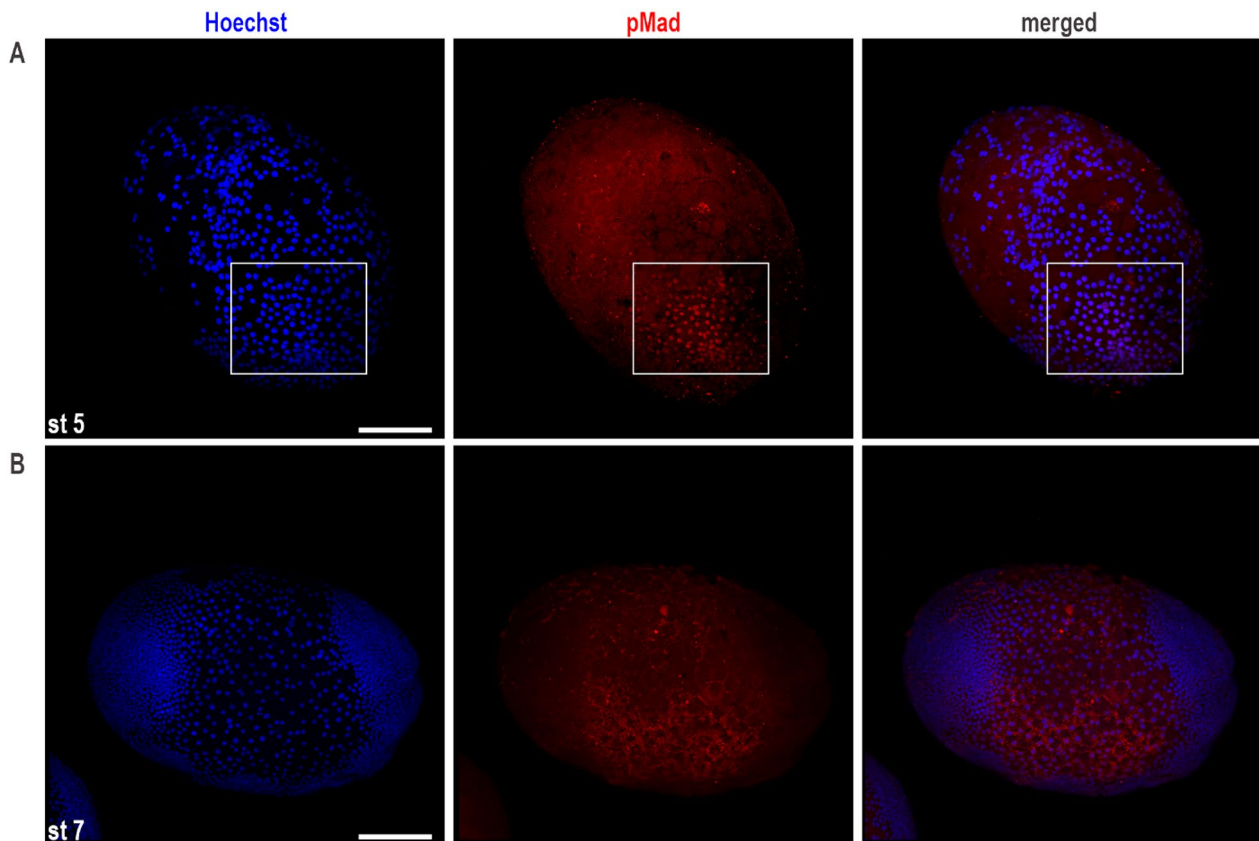


Fig. 8 Detection of BMP activity via pMAD staining among a cell cluster population. **A** At stage 5, pMAD staining is restricted to the population of the cell cluster (boxed region). **B** By stage 7, after these clusters of cells have been internalized, pMAD staining is spread around the ventral germband. Scale bars are 100 μm

Fertilization is thought to occur shortly after oviposition in *Ixodes* spp. [27]. However, it is important to note that *I. calcaratus* studied by Wagner [27] is now classified as *D. andersoni*, making our work the only study on any *Ixodes* spp. Although we did not observe the male and female pronuclei with DAPI staining, our timelapse video (S2) suggests syngamy occurs within the first hour post-egg laying. We observed early mitotic division at stage 1 (4 energids visible at ~ 12 h in the time-lapse video, Movie S2 and S3 frames 1–11). Rapid nuclear division took place at 24–48 h, resulting in a syncytial blastoderm. These early stages were missing in the previous studies [20–23]. The only other study that used early embryos was conducted on the camel tick, *Hyalomma dromedarii*, and suggested that the cleavage began within 3 hAEL [34] in this tick. However, cellularization was not investigated in any other tick species. Our data using embryo injection and whole-mount staining with WGA confirms that at least in *I. scapularis*, the early mitotic divisions are syncytial and settle the debate of holoblastic or syncytial division [20, 23, 29].

Different studies have suggested different cellularization times. For instance, Kocan et al., [35] suggested cellularization prior to egg laying in *I. scapularis*, whereas two other studies in *R. microplus* suggested cellularization at stage 1 or 6 [20, 23]. One of the limitations of these studies was the technical challenge of injecting tick embryos. We observed cellularization at 3–4 dAEL in Dextran-dye injections and WGA-FITC labeling, which corresponds to stage 4 in our staging system. We observed greater than 16 nuclei in 3 dAEL (Fig. 1C), pre-cellularized embryos, so our data suggests that cellularization occurs after the 16-cell stage, most likely 64–128 nuclei. In comparison, the spider mite *T. urticae* [36] and the spider *P. tepidariorum* [37] embryos were cellularized before the 8 and 16-cell stages, respectively. We were not successful in tracking cellularization with WGA-FITC injection into live eggs, unlike the *P. tepidariorum* embryos [33]. This may be due to WGA-FITC endocytosis and degradation in *I. scapularis* because *P. tepidariorum* has much faster embryonic development (~ 7 days), with significantly shorter staging times and cellularization within the

first 24 hAEL [25] which enabled successful real-time monitoring of cellularization in *P. tepidariorum*. In contrast, *I. scapularis* embryonic development is much longer (~35–40 days) [35] and our data). In *D. melanogaster*, the cellularization process takes approximately 1 h to complete. Given the much slower embryonic development of *I. scapularis*, we expect that several hours are needed for cellularization to complete.

In arachnids in the order *Araneae*, the process of gastrulation usually begins by the invagination of cells at the blastopore, followed by the formation of a primary thickening around the blastopore [31]. The blastopore and subsequently the primary thickening occur at the center of the germ disc. The germ disc is formed in some spider species by the migration of blastodermal cells towards one pole to form a cell-dense, dome-shaped disc which makes the embryonic primordium whereas the opposite pole will have a few scattered cells [31]. While a distinct germ-disc is present in some spiders [25, 38, 39], there are no visible germ discs in others such as the *Cupiennius salei* [26], *Acanthoscurria geniculata* (Pechmann, 2020) and *Tegenaria pagana* [40]. A distinct germ disc was not reported in *R. microplus* [20] or *D. andersoni* [21] ticks. Similarly, we did not observe a distinct germ disc in *I. scapularis*.

Similar to *D. andersoni*, the blastoderm forms around the periphery of the embryo surrounding the yolk granules. A cluster of cells, the cumulus mesenchymal cells, appears during stage 5. The cumulus of spiders plays an important role in establishing the embryonic body axes [25, 26] through the morphogenetic signals, such as the bone morphogenetic protein (BMP)-homolog, decapentaplegic (Dpp) [16, 19]. In *R. microplus*, anti-BMP antibodies bound to a cell cluster in the blastoderm, suggesting the presence of cumulus cells [20]. The cell cluster was also observed to migrate toward one pole of the blastoderm in both *R. microplus* and *D. andersoni*, based on fixed embryo staining methods. DAPI staining at stage 5 (6–7 dAEL), revealed a cluster of cells (Fig. 3B) that we presumed to be cumulus mesenchymal cells. Among this cluster of cells, we observed cells with large nuclei some of which were irregular in shape and had very loose chromatin structure. These large loosely packed chromatin nucleated cells will likely be specified as PGCs later. We detected BMP activity in a cluster of cells beneath the surface epithelial cell layer in embryos stage 5 embryos through antibody staining against the phosphorylated Mothers against dpp (pMAD) as has been done in other arthropods [16, 17, 19, 20]. In subsequent stages, the cluster of cells is observed at the posterior of the developing germ band through time-lapse imaging. However, this apparent migration to the posterior seems to be a result of embryo inversion, a process that internalizes

the yolk (Movie S3 frames 492–548). Similar observations have been reported in the harvestman *Phalangium opilio* where similar cell mass formed during late blastoderm stage appears to move posteriorly due to germ band extension rather than cell migration [41]. Further investigations would be valuable to determine whether this cell cluster relocation in *I. scapularis* involves active cell migration.

Unlike spiders, the ixodid tick body plan has two regions that consist of: (1) the capitulum containing the mouthparts and the basis capituli, which connects mouthparts to the body, and (2) the idiosoma, which arises from the podosoma (leg-containing segments) and opisthosoma (posterior growth zone). Similar to *D. andersoni* (Freisen et al., 2015), the anterior germ band gave rise to the segments of the podosoma and capitulum in *I. scapularis* and not the posterior growth zone. Like other chelicerates [20, 21, 25, 26, 36, 42], the posterior growth zone added more segments and thus extended the dorsal surface of the embryo. Following germ band retraction, the idiosoma was formed from the fusion and expansion of the opisthosomal and podosomal segments to surround the dorsal field cells, resulting in dorsal closure.

The bases of the chelicerae were situated laterally and posterior to the head lobes early in the development (stage 11) and moved to the midline by stage 12. Likewise, the palps underwent a similar rotation so that they were positioned laterally relative to the chelicerae. The movement of the chelicerae and palps resulted in the palp endites beneath the chelicerae, where they appeared to fuse to form the hypostome. The movement of the positioning of mouthparts agrees with what was previously observed in *D. andersoni* [21].

Primordial germ cell (PGC) specification studies in both vertebrate and invertebrate models have shown that germ line cells can be specified either early in development by maternally transmitted cytoplasmic factors (inheritance/preformed), or later in development by signaling factors from neighboring tissues (induction). While we did not investigate PGC formation, we expect that similar to the spider mite, *Tetranychus urticae*, the PGCs form later in development [43]. In *T. urticae*, no vasa expression was observed until after germband formation, suggesting the lack of maternally acquired vasa, a PGC marker [43], which is common in insects. Similarly, in the common house spider *P. tepidariorum*, transcript and protein expression patterns of *Pt-vasa* suggest that PGCs in this spider arise during late embryogenesis [44]. Since PGCs are the embryonic progenitor cells of sperm and eggs, which transmit genetic material between generations, these cells are ideal target for genetic manipulations, such as genome editing,

gene knock-in and transgenesis. Since cellularization in *I. scapularis* is completed by day 4 and germ band formation is apparent around day 10, it is plausible that PGCs arise after these events. Therefore, targeting embryos before cellularization (i.e., before 3 dAEL) may be the optimal window for germline transformation strategies. Transformation during the pre-cellularization stage could result in uniform integration across lineages, including germ cells. Whether the PGC formation in ticks follows preformation or induction mechanisms will be worth exploring.

Materials and methods

Tick samples and feeding

Pathogen-free, unfed adult *I. scapularis* ticks were purchased from the tick-rearing facility at the Oklahoma State University, Stillwater, Oklahoma, and kept in an incubator at 95% relative humidity (RH) and 20 °C in our laboratory at the University of Nevada, Reno (UNR). Ticks were blood-fed on New Zealand white rabbits. All procedures were approved by the Institutional Animal Care and Use Committee (IACUC) at UNR (IACUC # 21-01-1118).

Tick sample collection

Unfed females were placed on a rabbit with male ticks to mate and fully engorge. Replete females that fell off the rabbits were collected and placed in individual transparent plastic cups in a 20 °C incubator with 95% RH to promote egg laying or at 4 °C for long-term storage to prevent egg laying (up to 6 weeks). For the timing of embryonic development, eggs were collected daily into 1.7 ml tubes and stored in a 20 °C incubator until they reached the desired time point. The first time point was 0–6 h after egg laying (AEL) and collection occurred for multiple days until the larvae hatched.

Embryo staging

Embryos were collected at 0–6 h, 12 h, 24 h, and then at intervals of 24 h. The embryos were categorized into developmental stages (stage 0–15) according to Santos et al. [20] and our observations. Developmental times are reported as hours or days after egg laying (h/dAEL).

Embryo fixation

The embryos were placed in a cell strainer (70 µm; EASYstainer, Greiner Bio-One, North Carolina, USA) and washed in an 8% hypochlorite solution, with gentle agitation, using a fine paintbrush for 3 min. This treatment removes the thick layer of wax deposited on the eggs by the mother tick and softens the chorion. For young embryos (<2 dAEL), a 6% hypochlorite solution was used, and the wash duration was reduced to 2 min.

Subsequently, the embryos were rinsed with deionized (DI) water three times.

The embryos were transferred into a fresh 0.7 ml tube containing 100 µl of DI water using a fine paintbrush and subjected to heat shock at 90 °C for 3 min (2 min for younger embryos) in a thermal cycler. Immediately after heat shock, the embryos were snap-cooled at –20 °C for another 3 min (2 min for younger embryos), causing the chorion to crack. Once the DI water was thawed at RT, the embryos were transferred to a new 1.7 ml tube with a 1:1 ratio of heptane and 4% paraformaldehyde (PFA) in phosphate-buffered saline (PBS) (4% PFA in PBS) fixation solution. Fixation was done at RT on a vortex mixer at 300 rpm overnight.

After fixation, the lower PFA phase was removed and replaced with an equal volume of 100% methanol, and the tube was vigorously shaken for 1 min. The fixed embryos were stored at 4 °C for later imaging. Twenty embryos were used per time point. Embryos were collected from different females at the same egg-laying schedule.

Nuclear 4',6-diamidino-2-phenylindole dihydrochloride (DAPI) staining

Fixed embryos were prepared for staining by peeling the vitelline membrane with Tungsten needles (Fine Science Tools (Cat# 10,130-05) (Brady, 1965) or a Diamond knife (Trifacet, ME-131, Meyco) under a dissecting microscope. Peeled embryos were transferred to 1.7 ml microfuge tubes and rehydrated serially in 200 µl phosphate-buffer saline with 0.1% Tween-20 (PBS-T) and 75%, 50%, 25%, 0% methanol in PBS-T, followed by 100% PBS-T for 5 min each. The rehydrated embryos were incubated for 20 min. at RT with 50 µL of Invitrogen™ SlowFade™ Diamond Antifade Mountant with DAPI (ThermoFisher, Waltham, MA, USA) for at least 20 min. at RT for imaging. 10–15 embryos were imaged per time point.

Wheat germ agglutinin-fluorescein isothiocyanate (WGA-FITC) staining of membranes

A minimum of 10 (10–20) rehydrated, devitellinized embryos were prepared for staining using a method as described above for the DAPI staining. Instead of the addition of DAPI, the peeled embryos were incubated in 100 µl of WGA-FITC at a concentration of 1 µg/ml in PBS-T at RT for 1 h in the dark. After incubation, the WGA-FITC solution was removed, and the embryos were rinsed three times with PBS-T for 10 min each. Subsequently, 50 µL of Invitrogen™ SlowFade™ Diamond Antifade Mountant with DAPI (ThermoFisher, Waltham, MA, USA) was added to the embryos and incubated at RT for 20 min.

Microscopy and imaging

For staging, embryos were mounted onto concave microscope slides and a cover slip was placed on top of the well. Embryos were imaged using the Keyence BZ-X710 All-in-One Fluorescence Microscope. Images were analyzed and optimized using the Keyence BZ-X Analyzer software and ImageJ. Figure panels were made with Adobe Illustrator.

Microinjections with blue dextran 10,000 MW—Alexa Fluor 647

Embryos were treated as previously described [5, 6]. Briefly, chorion was removed by submerging embryos in 5% benzalkonium chloride for 5 min followed by two washes with deionized (DI) H₂O. The washed eggs were then treated with 5% NaCl for 3–5 min, washed twice with DI water, and kept in 1% NaCl until injected. Blue Dextran-Alexa Fluor 647 conjugate was diluted to 0.5 mg/mL and injected in live 1–9 AEL embryos. The embryos were imaged 16 h post-injection using a Keyence BZ-X710 Fluorescent microscope.

Phospho-mothers against decapentaplegic (pMAD) antibody staining

Fixed, devitellinized embryos stored in 100% methanol were gradually brought to PBS-T (0.1% Tween-20) as described above. The embryos were then washed in 100% PBS-T thrice for 5 min each and permeabilized in a detergent solution (SDS, Tween, EDTA, Tris-HCl, and NaCl) for 30 min. to facilitate antibody penetration. To reduce non-specific binding, the embryos were incubated for 5 h in a blocking solution consisting of 1% BSA + 5% goat serum in PBS-T. Afterwards, samples were incubated overnight in primary antibody, a rabbit phospho-SMAD1/5 (Ser463/465) antibody (#9516; Cell Signaling Technology, Boston, MA, USA) in the blocking solution at 1:100 dilution. The primary antibody was removed, and the embryos were rinsed and then washed with PBS-T 3 times for 15 min. each. The embryos were incubated in secondary antibody, goat anti-rabbit Alexa Fluor 555 conjugated (#4413S; Cell Signaling Technology, Boston, MA, USA) at 1:500 dilution for 2 h, rinsed with PBS-T and washed thrice with PBS-T for 15 min. each, and then counter-stained with Hoechst 33,342 (62,249; Thermofisher Scientific, MA, USA) at 1:2000 dilution for 30 min. The stained embryos were mounted and imaged in 70% glycerol with a Leica Stellaris 5 confocal microscope.

Time-lapse imaging

Eggs were collected early in the morning (deposited overnight), and the female ticks were left to lay more eggs.

Ticks were checked every 3–4 h for newly laid eggs. The eggs were transferred to a 35 mm plastic Petri dish and covered with CyGel (CY10500; BioStatus, Leicestershire, UK). A glass coverslip slide was gently placed on top and lightly pressed to secure the eggs. Next, halocarbon oil 700 was gently added to fill the space around the gel and coverslip to create an immersion environment and prevent desiccation. Images of the embryo were captured at 15 min intervals (i.e., every 900 s) throughout the embryonic development until larval hatching (40 days) using a Leica 205 FCA fluorescence stereomicroscope equipped with a Leica K3C camera. Time-lapse imaging was controlled using the time-lapse module of Leica Application Suite X software (LAS-X v.3.9). The resulting images were assembled into movies and annotated with ImageJ.

Supplementary Information

The online version contains supplementary material available at <https://doi.org/10.1186/s13227-025-00240-y>.

Supplementary material 1: Movie S1. Egg-laying female tick. Each time-lapse frame represents 5 mins. <https://www.dropbox.com/scl/fi/rgyqj4u4wfw6qt1zey4guq/Movie-S1-egg-laying.avi?rlkey=jnkk3uia6dggk4f6g7xv04fr8&st=yym18x1h&dl=0>.

Supplementary material 2: Movie S2. Timelapse of early embryonic development from 2 hours after egg laying until 3 days. https://www.dropbox.com/scl/fi/mu4mdsdvr40su1npdh8mm/Movie-S2-egg_dev_2_disc.avi?rlkey=bh1i3y0v660ju3311ojmp9cel&st=nxylf5c8&dl=0.

Supplementary material 3: Movie S3. Timelapse of Ixodes scapularis embryo development from ~6h hours until larval hatching. Each frame represents 15 minutes https://www.dropbox.com/scl/fi/jnc4mqniaaj8xnmzken2i/Movie-S3-lscap_egg_dev_day_1-23_fps8-1_frame_label.avi?rlkey=qf001c2icoqqfve2lgz3hyowh&st=vd314t4l&dl=0.

Supplementary material 4: Movie S4. Timelapse of Ixodes scapularis embryo development beginning with embryo 4 days after egg laying. Each frame represents 5 minutes https://www.dropbox.com/scl/fi/hh3qoxtztrjb4r169lrz3/Movie-S4-concatenated_16fps-2-frame_labels-1.avi?rlkey=liuzat05hxpqkktqnes120k2t&st=w0gtz0v&dl=0.

Supplementary material 5: Movie S5. Timelapse of Ixodes scapularis embryo development showing cumulus cells formation. Each frame is 10 minutes. https://www.dropbox.com/scl/fi/0n26jxf07zrss2itin4gf/Movie-S5-4-5D_3d-timelapse_concat-1_selection.avi?rlkey=3sst0g7xxnjq73xmxmf5mip3y&st=xobj5v6&dl=0.

Acknowledgements

We would like to thank Vitória Tobias Santos (Institut de Génétique Fonctionnelle de Lyon), Rodrigo Nunes da Fonseca (Instituto de Biodiversidade e Sustentabilidade (NUPEM), Universidade Federal do Rio de Janeiro, Campus Macaé), and Kevin J Friesen (MacEwan University) for their technical advice and sharing of protocols. We would like to thank members of the Gulia-Nuss lab- Drs. Isobel Ronai and Jeremiah Reyes for their technical assistance. We also thank Mr. Theodore Huff (Theodore G. Huff and Associates, LLC. Medical & Biological Illustration) for the illustrations.

Author contributions

I.A.H. and H.R.C. wrote the initial draft. I.A.H., A.B.N., M.G.-N., and P.P.S. wrote the final draft. I.A.H., H.R.C., A.S., and B.F. did DAPI staining, embryo staging, microscopy, and data analysis. J.W. generated the time-lapse videos, M.N.P. and M.M.V. conducted cellularization experiments. M.G.-N. and A.B.N. conceived the idea

and supervised the project. All authors provided critical feedback and helped shape the research, analysis and manuscript.

Funding

Confocal Microscopy was performed at the High Spatial and Temporal Imaging Core, of the Center of Biomedical Research Excellence (COBRE), University of Nevada, Reno, which is supported by the National Institutes of Health (NIGMS P20GM130459 Sub#5451 and P20GM130459 Sub#5452). This project was funded through National Institutes of Health grants R21AI128393 and R21 AI139778 to M.G.-N., National-Institute of Health grants R21AI176352 and R01AI172943 to M.G.-N., ABN, and MP, and a National Science Foundation Grant No. 2019609 to M.G.-N. and ABN. PPS was supported by National Science Foundation Grant No. 2016141.

Data availability

No datasets were generated or analysed during the current study.

Declarations

Competing interests

The authors declare no competing interests.

Received: 10 January 2025 Accepted: 11 April 2025

Published online: 25 April 2025

References

- Hoonstra D, Harms MG, Gauw SA, Wagemakers A, Azagi T, Kremer K, Sprong H, van den Wijngaard CC, Hovius JW. Ticking on Pandora's box: a prospective case-control study into 'other' tick-borne diseases. *BMC Infect Dis*. 2021;21(1):501. <https://doi.org/10.1186/s12879-021-06190-9>.
- CDC. (2023, September 11). *Tickborne diseases of the United States* | CDC. Centers for Disease Control and Prevention. <https://www.cdc.gov/ticks/diseases/index.html>
- Eisen L. Pathogen transmission in relation to duration of attachment by Ixodes scapularis ticks. *Ticks and Tick-Borne Dis*. 2018;9(3):535–42. <https://doi.org/10.1016/j.ttbdis.2018.01.002>.
- Kugeler KJ, Schwartz AM, Delorey MJ, Mead PS, Hinckley AF. Estimating the frequency of lyme disease diagnoses, united states, 2010–2018. *Emerg Infect Dis*. 2021;27(2):616–9. <https://doi.org/10.3201/eid2702.202731>.
- Sharma A, Pham M, Harrell RA, Nuss AB, Gulia-Nuss M. Embryo injection technique for gene editing in the black-legged tick *ixodes scapularis*. *JoVE*. 2022;187:e64142. <https://doi.org/10.3791/64142>.
- Sharma A, Pham MN, Reyes JB, Chana R, Yim WC, Heu CC, Kim D, Chaverra-Rodriguez D, Rasgon JL, Harrell RA, Nuss AB, Gulia-Nuss M. Cas9-mediated gene editing in the black-legged tick *Ixodes scapularis*, by embryo injection and ReMOT control. *iScience*. 2022;25(3):103781. <https://doi.org/10.1016/j.isci.2022.103781>.
- de Oliveira PR, Mathias MIC, Bechara GH. Vitellogenesis in the tick *Amblyomma triste* (Koch, 1844) (Acarina: Ixodidae). *Vet Parasitol*. 2007;143(2):134–9. <https://doi.org/10.1016/j.vetpar.2006.08.013>.
- Raikhel A. Reproductive system. In: Balashov IS, Balashov YS, Hoogstraal H, editors. *An Atlas of ixodid tick ultrastructure*. Bellingham: SPIE; 1983.
- Kiszewski AE, Matuschka F-R, Spielman A. Mating and spermiogenesis in Ixodid ticks. *Ann Rev Entomol*. 2001;46:167–82. <https://doi.org/10.1146/annurev.ento.46.1.167>.
- Diehl PA, Aeschlimann A, Obenchain FD. Tick reproduction: oogenesis and oviposition. In: *Physiology of ticks*. Oxford: Pergamon Press; 1982. p. 277–350.
- Lees AD, Beament JWL. An egg-waxing organ in ticks. *J Cell Sci*. 1948;3–89(7):291–332. <https://doi.org/10.1242/jcs.3-89.7.291>.
- Goroshchenko YL. Cytological investigations of certain properties of hematogenesis and karyologic systematic subdivision of argasid ticks. *Dokl. Soisk. Fluchen Step. Kand. Biol. Nauk, Leningrad*. 1965
- Araujo H, Fontenele MR, da Fonseca RN. Position matters: variability in the spatial pattern of BMP modulators generates functional diversity. *Genesis*. 2011;49(9):698–718. <https://doi.org/10.1002/dvg.20778>.
- Lynch JA, El-Sherif E, Brown SJ. Comparisons of the embryonic development of *Drosophila*, *Nasonia*, and *Tribolium*. *WIREs Dev Biol*. 2012;1(1):16–39. <https://doi.org/10.1002/wdev.3>.
- Lynch JA, Roth S. The evolution of dorsal–ventral patterning mechanisms in insects. *Genes Dev*. 2011;25(2):107–18. <https://doi.org/10.1101/gad.2010711>.
- Akiyama-Oda Y, Oda H. Axis specification in the spider embryo: *dpp* is required for radial-to-axial symmetry transformation and *sog* for ventral patterning. *Development*. 2006;133(12):2347–57. <https://doi.org/10.1242/dev.02400>.
- Akiyama-Oda Y, Oda H. Cell migration that orients the dorsoventral axis is coordinated with anteroposterior patterning mediated by hedgehog signaling in the early spider embryo. *Development*. 2010;137(8):1263–73. <https://doi.org/10.1242/dev.045625>.
- Campos-Ortega JA, Hartenstein V. *The embryonic development of drosophila melanogaster*. 1st ed. Berlin: Springer; 1985.
- Akiyama-Oda Y, Oda H. Early patterning of the spider embryo: a cluster of mesenchymal cells at the cumulus produces Dpp signals received by germ disc epithelial cells. *Development*. 2003;130(9):1735–47. <https://doi.org/10.1242/dev.00390>.
- Santos VT, Ribeiro L, Fraga A, de Barros CM, Campos E, Moraes J, Fontenele MR, Araújo HM, Feitosa NM, Logullo C, da Fonseca RN. The embryogenesis of the tick *Rhipicephalus (Boophilus) microplus*: the establishment of a new chelicerate model system: the embryogenesis of the tick. *Genesis*. 2013;51(12):803–18. <https://doi.org/10.1002/dvg.22717>.
- Friesen KJ, Dixon M, Lysyk TJ. Embryo development and morphology of the Rocky Mountain wood tick (*Acaris*: Ixodidae). *J Med Entomol*. 2016;53(2):279–89. <https://doi.org/10.1093/jme/tjv193>.
- Pressesky M. A study of the embryonic development of the Rocky Mountain spotted fever tick *Dermacentor andersoni* (Stiles) (*Acarina*, *Ixodidae*) [Master of Arts, University of Saskatchewan]. 1952. <http://hdl.handle.net/10388/etd-08032010-101524>
- Campos E, Moraes J, Façanha AR, Moreira E, Valle D, Abreu L, Manso PP, Nascimento A, Pelajo-Machado M, Lenzi H, Masuda A, Vaz IS, Logullo C. Kinetics of energy source utilization in *Boophilus microplus* (Castrini, 1887) (*Acaris*: *Ixodidae*) embryonic development. *Vet Parasitol*. 2006;138(3):349–57. <https://doi.org/10.1016/j.vetpar.2006.02.004>.
- McGregor AP, Hilbrant M, Pechmann M, Schwager EE, Prpic N-M, Damen WGM. *Cupiennius salei* and *Achaeareanea tepidariorum*: spider models for investigating evolution and development. *BioEssays*. 2008;30(5):487–98. <https://doi.org/10.1002/bies.20744>.
- Mittmann B, Wolff C. Embryonic development and staging of the cobweb spider *Parasteatoda tepidariorum* C. L. Koch, 1841 (syn.: *Achaeareanea tepidariorum*; *Araneomorphae*; *Theridiidae*). *Dev Genes Evol*. 2012;222(4):189–216. <https://doi.org/10.1007/s00427-012-0401-0>.
- Wolff C, Hilbrant M. The embryonic development of the central American wandering spider *Cupiennius salei*. *Front Zool*. 2011;8(1):15. <https://doi.org/10.1186/1742-9994-8-15>.
- Wagner J. Die Embryonalentwicklung von *Ixodes calcaratus*. 1894;24, 214–246
- Pham M, Sharma A, Nuss A, Gulia-Nuss M. Progress towards germline transformation of ticks. In: Benedict MQ, Scott MJ, editors. *Transgenic insects*. Wallingford: CABI; 2022.
- Fagotto F, Hess E, Aeschlimann A. The early embryonic development of the Argasid tick *Ornithodoros moubata* (Acarina: Ixodea: *Argasidae*). *Entomol Generalis*. 1988. <https://doi.org/10.1127/entom.gen/13/1988/1>.
- Foe VE, Alberts BM. Studies of nuclear and cytoplasmic behaviour during the five mitotic cycles that precede gastrulation in *Drosophila* embryogenesis. *J Cell Sci*. 1983;61(1):31–70. <https://doi.org/10.1242/jcs.61.1.31>.
- Hilbrant M, Damen WGM, McGregor AP. Evolutionary crossroads in developmental biology: The spider *Parasteatoda tepidariorum*. *Development*. 2012;139(15):2655–62. <https://doi.org/10.1242/dev.078204>.
- Holm Å (1940) Studien über die Entwicklung und Entwicklungsbiologie der Spinnen. *Zoologiska Bidrag från Uppsala* 19:1–214 Plates 1–11
- Pechmann M. Formation of the germ-disc in spider embryos by a condensation-like mechanism. *Front Zool*. 2016;13(1):35. <https://doi.org/10.1186/s12983-016-0166-9>.
- El Kammah KM, Adham FK, Tadross NR, Osman M. Embryonic development of the camel tick *hyalomma dromedarii* (Ixodidae: Ixodidae). *Int J Acarology*. 1982;8(1):47–54. <https://doi.org/10.1080/01647958208683276>.

35. Kocan KM, de la Fuente J, Coburn LA. Insights into the development of *Ixodes scapularis*: a resource for research on a medically important tick species. *Parasit Vectors*. 2015;8(1):592. <https://doi.org/10.1186/s13071-015-1185-7>.
36. Dearden PK, Donly C, Grbić M. Expression of pair-rule gene homologues in a chelicerate: early patterning of the two-spotted spider mite *Tetranychus urticae*. *Development*. 2002;129(23):5461–72. <https://doi.org/10.1242/dev.00099>.
37. Kanayama M, Akiyama-Oda Y, Oda H. Early embryonic development in the spider *Achaearanea tepidariorum*: Microinjection verifies that cellularization is complete before the blastoderm stage. *Arthropod Struct Dev*. 2010;39(6):436–45. <https://doi.org/10.1016/j.asd.2010.05.009>.
38. Chaw RC, Vance E, Black SD (2007) Gastrulation in the spider *Zygiella x-notata* involves three distinct phases of cell internalization. *Dev Dyn* 236:3484–3495. <https://doi.org/10.1002/dvdy.21371>
39. Edgar A, Bates C, Larkin K, Black S (2015) Gastrulation occurs in multiple phases at two distinct sites in *Latrodectus* and *Cheiracanthium* spiders. *EvoDevo* 6:33. <https://doi.org/10.1186/s13227-015-0029-z>
40. Propistsova EA, Gainett G, Chipman AD, Sharma PP, Gavish-Regev E. Shedding light on the embryogenesis and eye development of the troglophile cave spider *Tegenaria pagana* C. L. Koch, 1840 (*Araneae: Agelenidae*). *EvoDevo*. 2025;16(1):2. <https://doi.org/10.1186/s13227-025-00238-6>.
41. Gainett G, Crawford AR, Klementz BC, So C, Baker CM, Setton EVW, Sharma PP. Eggs to long-legs: embryonic staging of the harvestman *Phalangium opilio* (*Opiliones*), an emerging model arachnid. *Front Zool*. 2022;19(1):11. <https://doi.org/10.1186/s12983-022-00454-z>.
42. Grbic M, Khila A, Lee K-Z, Bjelica A, Grbic V, Whistlecraft J, Verdon L, Navajas M, Nagy L. Mity model: *Tetranychus urticae*, a candidate for chelicerate model organism. *BioEssays*. 2007;29(5):489–96. <https://doi.org/10.1002/bies.20564>.
43. Dearden P, Grbic M, Donly C. Vasa expression and germ-cell specification in the spider mite *Tetranychus urticae*. *Dev Genes Evol*. 2003;212(12):599–603. <https://doi.org/10.1007/s00427-002-0280-x>.
44. Schwager EE, Meng Y, Extavour CG. Vasa and piwi are required for mitotic integrity in early embryogenesis in the spider *Parasteatoda tepidariorum*. *Dev Biol*. 2015;402(2):276–90. <https://doi.org/10.1016/j.ydbio.2014.08.032>.

Publisher's Note

Springer Nature remains neutral with regard to jurisdictional claims in published maps and institutional affiliations.